COMPRESSED SENSING SUPER RESOLUTION OF COLOR IMAGES*

Wael Saafin[**1], *Miguel Vega*[2], *Rafael Molina*[1], *and Aggelos K. Katsaggelos*[3]

[1] Dept. of Computer Science and Artificial Intellegence, University of Granada, Granada, Spain.
[2] Dept. of Languages and Information Systems, University of Granada, Granada, Spain.
[3] Dept. of Electrical Engineering and Computer Science, Northwestern University, Evanston, USA
waelsaafin@hotmail.com, mvega@ugr.es, rms@decsai.ugr.es, aggk@eecs.northwestern.edu

ABSTRACT

In this work we estimate Super Resolution (SR) images from a sequence of true color Compressed Sensing (CS) observations. The red, green, blue (RGB) channels are sensed separately using a measurement matrix that can be synthesized practically. The joint optimization problem to estimate the registration parameters, and the High Resolution (HR) image is transformed into a sequence of unconstrained optimization sub-problems using the Alternate Direction Method of Multipliers (ADMM). A new, simple, and accurate, image registration procedure is proposed. The performed experiments show that the proposed method compares favorably to existing color CS reconstruction methods at unity zooming factor (P), obtaining very good performance varying P and the compression factor simultaneously. The algorithm is tested on real and synthetic images.

Index Terms— Super resolution, compressed sensing, color images, image reconstruction, image enhancement

1. INTRODUCTION

Compressive Sensing (CS) imaging simultaneously acquires and compresses images, thus reducing the acquisition time. CS image/video cameras (see [1–5]) have been applied to face recognition, biomedical imaging, and microscopy imaging [6–8].

CS has been applied to many typical image processing tasks. For instance, the problem of image deconvolution from CS measurements has been addressed in [9,10]. CS has also been used in SR problems. SR from a single CS image has been addressed in [11–13]. Gray scale image SR from multiple CS observations was proposed in [14–16], where CS and SR techniques were coupled using three different registration methods. The registration parameters were estimated at HR level from up-sampled versions of the reconstructed CS images in [14] and from the reconstructed HR image in [15]. In [16] the registration parameters were estimated at the Low resolution (LR) level from a down-sampled version of the estimated HR image.

CS reconstruction has been applied also to color images, when the three RGB channels are sensed separately. In [17] a method to obtain color images from CS observations has been proposed. The reconstruction process makes use of the correlation between the three color channels and is based on group sparse optimization. In [18], the single-pixel CS camera was combined with a Bayer color filter, to acquire CS color images, then joint sparsity models were applied to recover the three RGB channels. In [4] SR images are estimated from a single LR CS observation and applied to color images. In [13] CS video SR has been applied to spatial multiplexing cameras, and experimentally to color videos.

In this work we estimate color SR images from multiple observations acquired using CS techniques, and propose a new approach for image registration. The new Color Compressed Sensing Super Resolution (CCSSR) algorithm estimates motion vectors using LR reconstructed CS images.

The rest of this paper is organized as follows. The problem is modeled and formulated in Section 2. The estimation process is described in Section 3. Experimental analysis of the algorithm is presented in Section 4, and finally conclusions are stated in Section 5.

2. PROBLEM FORMULATION

Let us assume that we have access to a set of Q CS LR RGB color images of the form

$$\begin{aligned}\mathbf{y}_{cq} =& \mathbf{\Phi}_c \mathbf{A}\mathbf{H}_q\mathbf{C}(\mathbf{s}_q)\mathbf{x}_c + \mathbf{n}_{cq} \\ =& \mathbf{\Phi}_c \mathbf{B}_q(\mathbf{s}_q)\mathbf{x}_c + \mathbf{n}_{cq}\ , \text{ for } q = 1, \ldots, Q, \end{aligned} \tag{1}$$

where $c \in \{R, G, B\}$ denotes one of the three channels, $\mathbf{y}_{cq}$ is an $M \times 1$ vector representing the c channel of the q-th CS-LR observation, $\mathbf{\Phi}_c$ is the CS $M \times D$ measurement matrix corresponding to the c channel. The down-sampling matrix $\mathbf{A}$ is a $D \times N$ matrix, $D \leq N$, where $N = \mathrm{P}^2 D$ and $\mathrm{P} \geq 1$ is the zooming factor, in each dimension of the image. $\mathbf{H}_q$ is an $N \times N$ blurring matrix, which is assumed to be known. $\mathbf{C}(\mathbf{s}_q)$ is the $N \times N$ warping matrix for motion vector $\mathbf{s}_q = [\theta_q, c_q, d_q]^t$, where θ_q is the rotation angle, and c_q and d_q are, respectively, the horizontal and vertical translations of the q-th LR image with respect to the reference frame, $\mathbf{x}_c$ is an $N \times 1$ vector representing the c HR channel we want to estimate, and $\mathbf{n}_{cq}$ models the noise associated with the corresponding observation. We write $\mathbf{B}_q(\mathbf{s}_q) = \mathbf{A}\mathbf{H}_q\mathbf{C}(\mathbf{s}_q)$ for simplicity. We denote by F the compression factor of the measurement system, that is F$= M/D$, F≤ 1.

We assume in this paper that the LR images are sparse in a transformed domain. That is, $\mathbf{A}\mathbf{H}_q\mathbf{C}(\mathbf{s}_q)\mathbf{x}_c = \mathbf{W}\mathbf{a}_{cq}$, where $\mathbf{W}$ is a $D \times D$ transformation (wavelet) matrix, $\mathbf{a}_{cq}$ is the $D \times 1$ LR transformed coefficient vector corresponding to the c channel of the $q-$th observation. We assume that the $\mathbf{a}_{cq}$ vectors are sparse and then (see [16]) we recover them by solving

$$\begin{aligned} \min \quad & \sum_{c \in \{R,G,B\}} L(\mathbf{x}_c, \mathbf{a}_c) \\ \text{s.t.} \quad & \mathbf{B}_q(\mathbf{s}_q)\mathbf{x}_c = \mathbf{W}\mathbf{a}_{cq}, \text{ for } q = 1, \ldots, Q \text{ and } c \in \{R, G, B\}\,, \end{aligned} \tag{2}$$

*This paper has been supported by The European Union, Erasmus Mundus program, the Spanish Ministry of Economy and Competitiveness under project TIN2013-43880-R, the European Regional Development Fund (FEDER), and a Northwestern Catalyst Award. ** Corresponding author.

978-0-9928-6265-7/16/$31.00 ©2016 IEEE

where

$$L(\mathbf{x}_c, \mathbf{a}_c) = \frac{\eta}{2} \sum_{q=1}^{Q} \| \mathbf{\Phi W a}_c - \mathbf{y}_{cq} \|^2 + \tau \sum_{q=1}^{Q} \| \mathbf{a}_{cq} \|_1 + \alpha \, \mathbf{Q}(\mathbf{x}_c) \,, \tag{3}$$

with $\mathbf{a}_c = (\mathbf{a}_{c1}, \ldots, \mathbf{a}_{cQ})$, η, τ and α positive parameters, $\mathbf{Q}(\mathbf{x}_c)$ a regularization term which will be described soon, $\| \, . \, \|$ the Euclidean norm, and $\| \, . \, \|_1$ the $\ell 1$ norm.

3. CCSSR OPTIMIZATION APPROACH

Next we describe the optimization approach to the CCSSR problem. To convert the constrained optimization problem in (2) into an unconstrained one utilizing ADMM, we define the following augmented Lagrangian functionals

$$L(\mathbf{x}, \mathbf{a}, \mathbf{s}, \boldsymbol{\lambda}) = \sum_{c \in \{R,G,B\}} L_c(\mathbf{x}_c, \mathbf{a}_c, \mathbf{s}, \boldsymbol{\lambda}_c), \tag{4}$$

where

$$L_c(\mathbf{x}_c, \mathbf{a}_c, \mathbf{s}, \boldsymbol{\lambda}_c) = L(\mathbf{x}_c, \mathbf{a}_c) + \sum_{q=1}^{Q} \boldsymbol{\lambda}_{cq}^t (\mathbf{B}_q(\mathbf{s}_q)\mathbf{x}_c - \mathbf{W}\mathbf{a}_{cq}) + \frac{\beta}{2} \sum_{q=1}^{Q} \| \mathbf{B}_q(\mathbf{s}_q)\mathbf{x}_c - \mathbf{W}\mathbf{a}_{cq} \|^2, \tag{5}$$

and $L(\mathbf{x}_c, \mathbf{a}_c)$ has been defined in (3), $\mathbf{s} = (\mathbf{s}_1, \ldots, \mathbf{s}_Q)$ is the set of motion vectors, $\boldsymbol{\lambda}_c = (\boldsymbol{\lambda}_{c1}, \ldots, \boldsymbol{\lambda}_{cQ})$ is the set of $D \times 1$ Lagrangian multiplier vectors $\boldsymbol{\lambda}_{cq}$, and β is a positive parameter. The ADMM leads to the following sequence of iterative unconstrained problems,

$$\mathbf{x}_c^{k+1} = \arg\min_{\mathbf{x}_c} L_c(\mathbf{x}_c, \mathbf{a}_c^k, \mathbf{s}^k, \boldsymbol{\lambda}_c^k) \,, \tag{6}$$

$$\mathbf{a}_c^{k+1} = \arg\min_{\mathbf{a}_c} L_c(\mathbf{x}_c^{k+1}, \mathbf{a}_c, \mathbf{s}^k, \boldsymbol{\lambda}_c^k) \tag{7}$$

$$\mathbf{s}^{k+1} = \arg\min_{\mathbf{s}} \sum_{c \in \{R,G,B\}} L_c(\mathbf{x}_c^{k+1}, \mathbf{a}_c^{k+1}, \mathbf{s}, \boldsymbol{\lambda}_c^k) \tag{8}$$

$$\boldsymbol{\lambda}_{cq}^{k+1} = \boldsymbol{\lambda}_{cq}^k - \beta[\mathbf{B}_q(\mathbf{s}_q^{k+1})\mathbf{x}_c^{k+1} - \mathbf{W}\mathbf{a}_{cq}^{k+1}] \,, \;\; q = 1, \ldots, Q, \tag{9}$$

where k is the iteration index. Notice that according to the ADMM formulation, $\mathbf{B}_q(\mathbf{s}_q)$ in (2) should not depend on the iteration index, as is not the case here. However, we have not encountered any convergence issues with this iterative procedure.

The regularization term $\mathbf{Q}(\mathbf{x}_c)$ is given by

$$\mathbf{Q}(\mathbf{x}_c) = \sum_{d \in \Delta} \sum_{i=1}^{N} \log_\epsilon(|\omega_d^{\mathbf{x}_c}(i)|) \,, \tag{10}$$

which replaces $\log |\omega_d^{\mathbf{x}_c}(i)|$ by its robust version

$$\log_\epsilon(|\omega_d^{\mathbf{x}_c}(i)|) = \begin{cases} \log(|\omega_d^{\mathbf{x}_c}(i)|), & \text{for } |\omega_d^{\mathbf{x}_c}(i)| \geq \epsilon \\ \frac{|\omega_d^{\mathbf{x}_c}(i)|^2}{2\epsilon^2} - (\frac{1}{2} - \log(\epsilon)), & \text{for } 0 \leq |\omega_d^{\mathbf{x}_c}(i)| \leq \epsilon \end{cases} \tag{11}$$

to avoid the singularity at zero. $\omega_d^{\mathbf{x}_c}(i)$ is the i-th pixel of the filtered channel, that is,

$$\boldsymbol{\omega}_d^{\mathbf{x}_c} = \mathbf{F}_d \mathbf{x}_c \,, \tag{12}$$

where $\mathbf{F}_d$ is a high-pass filter operator, and the index $d \in \Delta$ denotes one of the filters in Δ. In this paper we have used $\Delta = \{h, v, hv, vh, hh, vv\}$, where h, v represent the first order horizontal and vertical difference filters, hv and vh the first order differences along diagonals, and hh and vv the horizontal and vertical second order differences.

For the regularization term $\mathbf{Q}(\mathbf{x}_c)$ in (10), we can write

$$\mathbf{Q}(\mathbf{x}_c) \leq R(\mathbf{x}_c, \boldsymbol{\xi}_c) = \frac{1}{2} \sum_{d \in \Delta} \mathbf{x}_c^t \mathbf{F}_d^t \mathbf{\Omega}_d \mathbf{F}_d \mathbf{x}_c - \sum_{d \in \Delta} \sum_{i=1}^{N} \rho_\epsilon^*(\frac{1}{2}\xi_{cd}(i)) \tag{13}$$

where $\boldsymbol{\xi} = (\boldsymbol{\xi}_{c1}, \ldots, \boldsymbol{\xi}_{cQ})$, $\boldsymbol{\xi}_{cq} = (\xi_{cq}(1), \ldots, \xi_{cq}(N))$ for $q = 1, \ldots, Q$, with all its components positive, $\mathbf{\Omega}_d$ is a diagonal matrix with entries

$$\Omega_{cd}(i,i) = \xi_{cd}(i) \,. \tag{14}$$

For a given $\mathbf{x}_c$ the inequality in (13) becomes an equality if $\rho_\epsilon^*(\frac{1}{2}\xi_{cd}(i))$ is defined by (see [19] for details),

$$\xi_{cd}^{\mathbf{x}_c}(i) = \min(\frac{1}{|\omega_d^{\mathbf{x}_c}(i)|^2}, \frac{1}{\epsilon^2}) = \begin{cases} \frac{1}{|\omega_d^{\mathbf{x}_c}(i)|^2}, & \text{for } |\omega_d^{\mathbf{x}_c}(i)| \geq \epsilon \\ \frac{1}{\epsilon^2}, & \text{for } 0 \leq |\omega_d^{\mathbf{x}_c}(i)| \leq \epsilon \end{cases} \tag{15}$$

where $\omega_d^{\mathbf{x}_c}(i)$ is defined from $\mathbf{x}_c$ in (12). Then we can apply a standard Majorization-Minimization method [20]. Given $\mathbf{x}_c^k, \mathbf{a}_c^k, \mathbf{s}^k$ and defining

$$L_c^k(\mathbf{x}_c) = \frac{\beta}{2} \sum_q \| \mathbf{B}_q(\mathbf{s}_q^k)\mathbf{x}_c - \mathbf{W}\mathbf{a}_{cq}^k \|^2 + \sum_q \boldsymbol{\lambda}_{cq}^{k\,t} (\mathbf{B}_q(\mathbf{s}_q^k)\mathbf{x}_c - \mathbf{W}\mathbf{a}_{cq}^k) \tag{16}$$

it can be easily shown that

$$L_c^k(\mathbf{x}_c^k) + \alpha \mathbf{Q}(\mathbf{x}_c^k) \geq L_c^k(\mathbf{x}_c^{k+1}) + \alpha \mathbf{Q}(\mathbf{x}_c^{k+1}) \tag{17}$$

where

$$\mathbf{x}_c^{k+1} = \arg\min_{\mathbf{x}_c} \left\{ \frac{\beta}{2} \sum_q \| \mathbf{B}_q(\mathbf{s}_q^k)\mathbf{x}_c - \mathbf{W}\mathbf{a}_{cq} \|^2 + \alpha R(\mathbf{x}_c, \boldsymbol{\xi}_c^{\mathbf{x}_c^k}) + \sum_q \boldsymbol{\lambda}_{cq}^{k\,t} (\mathbf{B}_q(\mathbf{s}_q^k)\mathbf{x}_c - \mathbf{W}\mathbf{a}_{cq}^k) \right\}. \tag{18}$$

From (18), the optimization step in (6) produces the following solution for $\mathbf{x}_c^{k+1}$

$$\mathbf{x}_c^{k+1} = \left[\beta \sum_q \mathbf{B}^{k\,t}{}_q(\mathbf{s}_q^k)\mathbf{B}_q^k(\mathbf{s}_q^k) + \alpha \sum_{d \in \Delta} \mathbf{F}_d^t \mathbf{\Omega}_{cd}^k \mathbf{F}_d \right]^{-1} \times \sum_q \mathbf{B}_q^k(\mathbf{s}_q^k)^t \left[\beta \mathbf{W}\mathbf{a}_{cq}^k - \lambda_{cq}^k \right] \tag{19}$$

where

$$\Omega_{cd}^k(i,i) = \min(1/|\omega_d^{\mathbf{x}_c^k}(i)|^2, 1/\epsilon^2). \tag{20}$$

The optimization step in (7) for each $\mathbf{a}_{cq}$ produces

$$\mathbf{a}_{cq}^{k+1} = \arg\min_{\mathbf{a}_{cq}} \left\{ \frac{\eta}{2} \| \mathbf{\Phi W a}_{cq} - \mathbf{y}_{cq} \|^2 + \tau \| \mathbf{a}_{cq} \|_1 + \frac{\beta}{2} \| \mathbf{B}_q^k(\mathbf{s}_q^k)\mathbf{x}_c^{k+1} - \mathbf{W}\mathbf{a}_{cq} \|^2 - \boldsymbol{\lambda}_{cq}^{k\,t} (\mathbf{B}_q^k(\mathbf{s}_q^k)\mathbf{x}_c - \mathbf{W}\mathbf{a}_{cq}) \right\} \tag{21}$$

which is equivalent to

$$\mathbf{a}_{cq}^{k+1} = \arg\min_{\mathbf{a}_{cq}} \Big\{ \frac{\eta}{2} \parallel \mathbf{\Phi W a}_{cq} - \mathbf{y}_{cq} \parallel^2 + \frac{\beta}{2} \parallel \mathbf{B}_q^k(\mathbf{s}_q^k)\mathbf{x}_c^{k+1} - \boldsymbol{\lambda}_{cq}^k - \mathbf{W a}_{cq} \parallel^2 + \tau \parallel \mathbf{a}_{cq} \parallel_1 \Big\}. \quad (22)$$

The above equation can be rewritten as

$$\mathbf{a}_{cq}^{k+1} = \arg\min_{\mathbf{a}_{cq}} \parallel \mathbf{\Phi}_c' \mathbf{W a}_{cq} - \mathbf{J}' \parallel^2 + \tau \parallel \mathbf{a}_{cq} \parallel_1, \quad (23)$$

where

$$\mathbf{J}' = \begin{bmatrix} \sqrt{\frac{\eta}{2}}\mathbf{y}_{cq} \\ \sqrt{\frac{\beta}{2}}(\mathbf{B}_q^k(\mathbf{s}_q^k)\mathbf{x}_c^{k+1} - \boldsymbol{\lambda}_{cq}^k) \end{bmatrix} \quad \text{and} \quad \mathbf{\Phi}' = \begin{bmatrix} \sqrt{\frac{\eta}{2}}\mathbf{\Phi}_c \\ \sqrt{\frac{\beta}{2}}\mathbf{I} \end{bmatrix} \quad (24)$$

with $\mathbf{I}$ the $D \times D$ identity matrix.

The above optimization problem can be solved using the algorithm in [21].

Instead of estimating the registration parameters by solving (8), we could find their down-sampled versions by solving

$$\mathbf{s}_{Lq}^{k+1} = \arg\min_{\mathbf{s}_{Lq}} \frac{\beta'}{2} \sum_{c\in\{R,G,B\}} \parallel \mathbf{C}'(\mathbf{s}_{Lq})\mathbf{W a}_{cr}^{k+1} - \mathbf{W a}_{cq}^{k+1} \parallel^2, \quad (25)$$

where $\mathbf{C}'(\mathbf{s}_{Lq})$ is a $D \times D$ warping matrix, β' is a positive parameter, and r denotes the LR reference image. However, instead of minimizing (25), we solve the following joint estimation problem

$$\mathbf{s}_{Lq}^{k+1} = \arg\min_{\mathbf{s}_{Lq}} \frac{\beta'}{2} \parallel \mathbf{C}'(\mathbf{s}_{Lq})\mathbf{z}^{k+1} - \mathbf{z}_q^{k+1} \parallel^2, \quad (26)$$

where $\mathbf{z} = Y(\mathbf{W a}_r)$, $\mathbf{z}_q = Y(\mathbf{W a}_q)$, and $Y(\mathbf{a})$ is calculated using

$$Y(\mathbf{a}) = 0.2989\,\mathbf{a}_R + 0.5870\,\mathbf{a}_G + 0.1140\,\mathbf{a}_B, \quad (27)$$

where $\mathbf{a}_R, \mathbf{a}_G$, and $\mathbf{a}_B$ are the R, G, and B channels of the transformed coefficient vector.

Notice that the warped LR observation $\mathbf{C}'(\mathbf{s}_{Lq})\mathbf{z}$ is equivalent to the LR version of $\mathbf{C}_q(\mathbf{s}_q)\mathbf{x}_c$, and it can be approximated by expanding it into its first-order Taylor series around the previous value $\mathbf{s}_{Lq}^k$. Hence we have (see [16, 22, 23])

$$\mathbf{C}'(\mathbf{s}_{Lq}^{k+1})\mathbf{z}^{k+1} \approx \mathbf{C}'(\mathbf{s}_{Lq}^k)\mathbf{z}^{k+1} + \Big[\mathbf{N}_{q1}(\mathbf{s}_{Lq}^k)\mathbf{z}^{k+1}, \mathbf{N}_{q2}(\mathbf{s}_{Lq}^k)\mathbf{z}^{k+1}, \mathbf{N}_{q3}(\mathbf{s}_{Lq}^k)\mathbf{z}^{k+1}\Big](\mathbf{s}_{Lq}^{k+1} - \mathbf{s}_{Lq}^k), \quad (28)$$

where $\mathbf{N}_i(\mathbf{s}_{Lq}^k)\mathbf{z}^{k+1}$ can be calculated using

$$\Big[\mathbf{N}_1(\mathbf{s}_{Lq}^k)\mathbf{z}, \mathbf{N}_2(\mathbf{s}_{Lq}^k)\mathbf{z}, \mathbf{N}_3(\mathbf{s}_{Lq}^k)\mathbf{z}\Big] = \Big[(\mathbf{P}_1(\mathbf{s}_{Lq}^k)\mathbf{M}_1(\mathbf{s}_{Lq}^k) + \mathbf{P}_2(\mathbf{s}_{Lq}^k)\mathbf{M}_2(\mathbf{s}_{Lq}^k), \mathbf{M}_1(\mathbf{s}_{Lq}^k), \mathbf{M}_2(\mathbf{s}_{Lq}^k)\Big], \quad (29)$$

with

$$\begin{aligned}
\mathbf{M}_1(\mathbf{s}_{Lq}^k) &= (\mathbf{I} - \mathbf{D}_{\mathbf{b}_q(\mathbf{s}_{Lq})})(\mathbf{L}_{tr(s_{Lq})} - \mathbf{L}_{tl(s_{Lq})}) \\
&\quad + \mathbf{D}_{\mathbf{b}_q(\mathbf{s}_{Lq})}(\mathbf{L}_{br(s_{Lq})} - \mathbf{L}_{bl(s_{Lq})}) \\
\mathbf{M}_2(\mathbf{s}_{Lq}^k) &= (\mathbf{I} - \mathbf{D}_{\mathbf{a}_q(\mathbf{s}_{Lq})})(\mathbf{L}_{bl(s_{Lq})} - \mathbf{L}_{tl(s_{Lq})}) \\
&\quad + \mathbf{D}_{\mathbf{a}_q(\mathbf{s}_{Lq})}(\mathbf{L}_{br(s_{Lq})} - \mathbf{L}_{tr(s_{Lq})}) \\
\mathbf{P}_1(\mathbf{s}_{Lq}^k) &= -[\mathbf{D}_{\mathbf{u}}\sin(\theta_q^k) + \mathbf{D}_{\mathbf{v}}\cos(\theta_q^k)] \\
\mathbf{P}_2(\mathbf{s}_{Lq}^k) &= [\mathbf{D}_{\mathbf{u}}\cos(\theta_q^k) - \mathbf{D}_{\mathbf{v}}\sin(\theta_q^k),
\end{aligned} \quad (30)$$

Algorithm 1 Color CSSR Algorithm (CCSSR).

Require: Values $\alpha, \beta, \tau, \eta$
Initialize $\mathbf{a}^0, \mathbf{s}^0, \boldsymbol{\lambda}^0, \mathbf{\Omega}^0 = \{\mathbf{\Omega}_d^0, d \in \Delta\}$
$k = 0$
while convergence criterion is not met **do**
1. for $c \in \{R, G, B\}$
i Calculate $\mathbf{x}_c^{k+1}$ by solving (19)
ii For $d \in \Delta$, calculate $\mathbf{\Omega}_{cd}^{k+1}$ using (20)
iii For $q = 1, \ldots, Q$, calculate $\mathbf{a}_{cq}^{k+1}$ using (23)
iv For $q = 1, \ldots, Q$, update $\boldsymbol{\lambda}_{cq}^{k+1}$ using (9)
2. For $q = 1, \ldots, Q$, calculate $\mathbf{s}_q^{k+1}$ using (33)
3. Set $k = k + 1$
end while
return $\mathbf{x} = [\mathbf{x}_R, \mathbf{x}_G, \mathbf{x}_B]$

where $\mathbf{D}_{\mathbf{u}}$ and $\mathbf{D}_{\mathbf{v}}$ are diagonal matrices whose diagonals are the vectors $\mathbf{u}$ and $\mathbf{v}$, respectively. They represent the pixel coordinates in $\mathbf{z}$. Matrices $\mathbf{L}_\kappa$ with $\kappa \in \{bl(\mathbf{s}_{Lq}), br(\mathbf{s}_{Lq}), tl(\mathbf{s}_{Lq}), tr(\mathbf{s}_{Lq})\}$ are constructed in such a way that the product $\mathbf{L}_\kappa\mathbf{z}$ produces respectively pixels at the bottom-left, bottom-right, top-left, and top-right, pixel locations in $\mathbf{z}_q$. Substituting (28) into (26), we obtain the final update equation as follows

$$\mathbf{s}_{Lq}^{k+1} = \mathbf{s}_{Lq}^k + \Big[\mathbf{\Lambda}_q^k\Big]^{-1} \Upsilon_q^k, \quad (31)$$

where $\mathbf{\Lambda}_q^k$ and Υ_q^k correspond to the q-th observation at the k-th iteration, with respectively $(i, j) \in \{1, 2, 3\}$ element and $i \in \{1, 2, 3\}$ element given by

$$\begin{aligned}
\Lambda_{qij}^k &= \Big[\mathbf{N}_i(\mathbf{s}_{Lq}^k)\mathbf{z}^{k+1}\Big]^t \mathbf{N}_j(\mathbf{s}_{Lq}^k)\mathbf{z}^{k+1}, \\
\Upsilon_{qi}^k &= \Big[\mathbf{N}_i(\mathbf{s}_{Lq}^k)\mathbf{z}^{k+1}\Big]^t (\mathbf{z}_q^{k+1} - \mathbf{N}_i(\mathbf{s}_{Lq}^k)\mathbf{z}^{k+1}).
\end{aligned} \quad (32)$$

If $\mathbf{s}_{Lq}^{k+1} = [\theta_{Lq}, c_{Lq}, d_{Lq}]^t$ then the HR motion vector is approximated by

$$\mathbf{s}_q^{k+1} = [\theta_{Lq}, \mathrm{P}{\cdot}c_{Lq}, \mathrm{P}{\cdot}d_{Lq}]^t \quad (33)$$

The complete CCSSR algorithm is presented in Algorithm 1.

4. EXPERIMENTAL RESULTS

To analyze the behavior of the proposed CCSSR method we carried out a set of experiments on the images shown in Figures 1(a-c). The images have been warped, then degraded by Gaussian blurs of different known variances and down-sampled. The LR RGB channels have been compressed separately using a circulant Toeplitz matrix, to serve as a measurement matrix which could be practically synthesized, following the Bernoulli probability distribution. White Gaussian noise, with SNR=40 dB, has been finally added to the compressed channels.

Figures 1(d,e) show respectively examples of a simulated LR and a CS-LR observations for the Barbara image using motion vector $\mathbf{s} = [.1222, -2, 3]^t$, blur variance 7, P= 2 and F=0.5. We used a 3-level Haar wavelet transform as the transform basis W, Peak Signal to Noise Ratio (PSNR) as the performance measure, and $\frac{norm(\mathbf{x}^k - \mathbf{x}^{k-1})}{norm(\mathbf{x}^{k-1})} \leq 10^{-3}$ as the stopping criterion.

In the first experiment Q=3 observations and a zooming factor P=1 have been used in order to compare our method with the following CS reconstruction methods: Nagesh et. al [18] (Na) , Wakin et

(a) (b)

(c) (d) (e)

Fig. 1. Original Images (a) Barbara, (b) Lena, and (c) Peppers. (d) Simulated LR Barbara image ($\mathbf{s} = [.1222, -2, 3]^t$, blur variance 7, P=2), (e) simulated CS observation (F=0.5, SNR=40 dB). The black line represents the added zero-valued entries to illustrate a square image.

al [24] (Wa), Majumdar L2,1 (L1), L2,0.4 (L4), and SL2,0 (SL) [17]. Results are tabulated in Table 1.

Table 1. Performance comparison for CS algorithms with proposed algorithm, for CCSSR P=1.0, Q=3. In bold are the highest PSNR values.

Image	Alg / F	Na	Wa	L1	L4	SL	CCSSR
		PSNR Values					
Barbara	.1	25.1	24.8	26.1	**26.7**	26.5	21.3
	.2	27.1	26.6	28.0	28.5	28.3	**29.9**
	.3	28.8	27.9	29.3	30.0	29.7	**34.0**
Lena	.1	26.1	25.9	27.0	**27.6**	27.5	25.8
	.2	28.3	27.7	29.0	29.7	29.5	**31.6**
	.3	30.0	29.2	30.7	31.7	31.1	**37.0**
Peppers	.1	25.0	24.5	25.6	**26.3**	26.0	24.8
	.2	27.1	26.1	27.9	28.5	28.1	**32.5**
	.3	29.8	28.1	30.5	21.4	30.9	**35.2**

Figure 2 shows a comparison between CS algorithms and the proposed CCSSR algorithm. PSNR vs F curves are shown for P=1.0 and Q=3 for all algorithms. The performance of the proposed CCSSR outperforms others at practical **F**s. However, for $\mathbf{F} = 0.1$ the performance measure shows values similar to other works.

In the second experiment we investigate the performance of the proposed CCSSR algorithm for practical P and F values. For all images we used Gaussian blur of variance 5, P=4, SNR=40dB, and Q=3. The results are shown in Figure 3 for the three images used in our study and different values of F.

Figures 4(a,b) show the reconstructed peppers images using

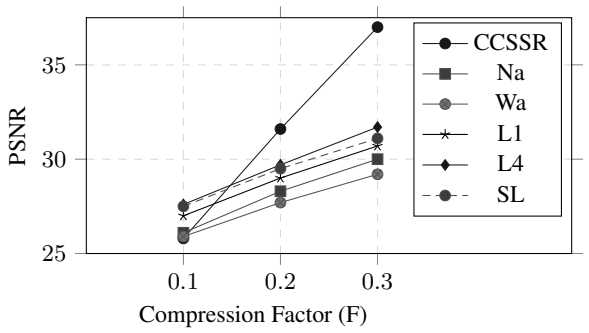

Fig. 2. Comparison between CS algorithms and CCSSR algorithm for the Lena image. For CCSSR, P=1, Q=3.

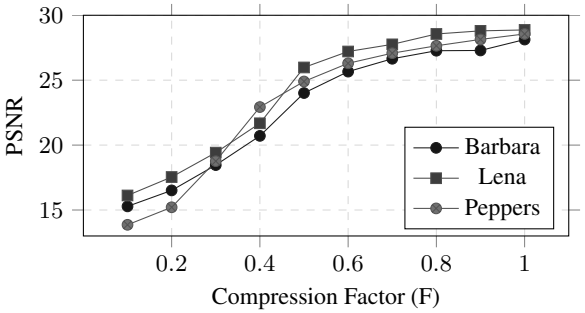

Fig. 3. Performance Measure of proposed CCSSR vs F. P=4, Blur Var=5, SNR=40dB, Q=3.

(a) (b)

Fig. 4. Reconstructed Peppers Images using CCSSR algorithm. F=0.6, Blur Var=5, SNR=40dB, and Q=3. (a) P=2, (b) P=4,

CCSSR (F=0.6, Blur Var=5, SNR=40dB, and Q=3), for P=2 and P=4, respectively. Figure 5(b) shows the result obtained using the CCSSR (F=0.8, P=2) from 16 synthetically generated CS observations from a sequence of 16 real LR input images of a toy whose first 4 images are shown in 5(a).

5. CONCLUSIONS

In this work we have estimated HR color images from multiple CS LR acquired images. The separately sensed channels are utilized in a joint registration estimation procedure which effectively and accurately estimates the registration parameters. This novel estimation is based on the LR estimated images instead of the HR ones. The

(a) (b)

Fig. 5. Estimation of HR image from synthetically CS real images using CCSSR algorithm. (a) The first 4 of 16 input images, (b) Output image (F=0.8, P=2)

estimated HR images compare favorably to those obtained by CS methods which correlate the color channels.

6. REFERENCES

[1] M.F. Duarte, M.A. Davenport, D. Takhar, J.N. Laska, Ting Sun, K.F. Kelly, and R.G. Baraniuk, "Single-pixel imaging via compressive sampling," *Signal Processing Magazine, IEEE*, vol. 25, no. 2, pp. 83–91, March 2008.

[2] W. L. Chan, K. Charan, D. Takhar, K. F. Kelly, R.G. Baraniuk, and D.M. Mittleman, "A single-pixel terahertz imaging system based on compressed sensing," *Applied Physics Letters*, vol. 93, no. 12, pp. 121105–121105–3, Sep 2008.

[3] A. Heidari and D. Saeedkia, "A 2d camera design with a single-pixel detector," in *Infrared, Millimeter, and Terahertz Waves, 2009. IRMMW-THz 2009. 34th International Conference on*, Sept 2009, pp. 1–2.

[4] A.C. Sankaranarayanan, C. Studer, and R.G. Baraniuk, "Cs-muvi: Video compressive sensing for spatial-multiplexing cameras," in *Computational Photography (ICCP), 2012 IEEE International Conference on*, April 2012, pp. 1–10.

[5] R. Koller, L. Schmid, N. Matsuda, T. Niederberger, L. Spinoulas, O. Cossairt, G. Schuster, and A. K. Katsaggelos, "High spatio-temporal resolution video with compressed sensing," *Opt. Express*, vol. 23, no. 12, pp. 15992–16007, Jun 2015.

[6] M. Fornasier and H. Rauhut, "Compressive sensing," in *Handbook of mathematical methods in imaging*, pp. 187–228. Springer, 2011.

[7] Y. C. Eldar and G. Kutyniok, *Compressed sensing: theory and applications*, Cambridge University Press, 2012.

[8] H.P. Babcock, J.R. Moffitt, Y. Cao, and X. Zhuang, "Fast compressed sensing analysis for superresolution imaging using l1-homotopy," *Optics Express*, vol. 21, no. 23, pp. 28583–28596, 2013.

[9] L. Spinoulas, B. Amizic, M. Vega, R. Molina, and A.K. Katsaggelos, "Simultaneous bayesian compressive sensing and blind deconvolution," in *Signal Processing Conference (EUSIPCO), 2012 Proceedings of the 20th European*, Aug 2012, pp. 1414–1418.

[10] B. Amizic, L. Spinoulas, R. Molina, and A.K. Katsaggelos, "Compressive blind image deconvolution," *Image Processing, IEEE Transactions on*, vol. 22, no. 10, pp. 3994–4006, Oct 2013.

[11] C. He, L. Liu, L. Xu, M. Liu, and M. Liao, "Learning based compressed sensing for sar image super-resolution," *Selected Topics in Applied Earth Observations and Remote Sensing, IEEE Journal of*, vol. 5, no. 4, pp. 1272–1281, 2012.

[12] S. Yang, F. Sun, M. Wang, Z. Liu, and L. Jiao, "Novel super resolution restoration of remote sensing images based on compressive sensing and example patches-aided dictionary learning," in *Multi-Platform/Multi-Sensor Remote Sensing and Mapping (M2RSM), 2011 International Workshop on*. IEEE, 2011, pp. 1–6.

[13] P. Sen and S. Darabi, "Compressive image super-resolution," in *Signals, Systems and Computers, 2009 Conference Record of the Forty-Third Asilomar Conference on*, Nov 2009, pp. 1235–1242.

[14] W. Saafin, M. Vega, R. Molina, and A. K. Katsaggelos, "Image super-resolution from compressed sensing observations," in *Image Processing (ICIP), 2015 IEEE International Conference on*, Sept 2015, pp. 4268–4272.

[15] W. Saafin, S. Villena, M. Vega, R. Molina, and A. K. Katsaggelos, "Pmmw image super resolution from compressed sensing observations," in *Signal Processing Conference (EUSIPCO), 2015 23rd European*, Aug 2015, pp. 1815–1819.

[16] W. AlSaafin, S. Villena, M. Vega, R. Molina, and A.K. Katsaggelos, "Compressive sensing super resolution from multiple observations with application to passive millimeter wave images," *Digital Signal Processing*, pp. 180–190, 2016.

[17] A. Majumdar and R. Ward, "Compressed sensing of color images," *Signal Processing*, vol. 90, no. 12, pp. 3122–3127, 2010.

[18] P. Nagesh and B. Li, "Compressive imaging of color images," in *Acoustics, Speech and Signal Processing, 2009. ICASSP 2009. IEEE International Conference on*. IEEE, 2009, pp. 1261–1264.

[19] S Derin Babacan, Rafael Molina, Minh N Do, and Aggelos K Katsaggelos, "Bayesian blind deconvolution with general sparse image priors," in *Computer Vision–ECCV 2012*, pp. 341–355. Springer, 2012.

[20] K. Lange, *Optimization*, Springer-Verlag, 2013.

[21] S-J Kim, K. Koh, M. Lustig, S. Boyd, and D. Gorinevsky, "An interior-point method for large-scale l1-regularized least squares," *Selected Topics in Signal Processing, IEEE Journal of*, vol. 1, no. 4, pp. 606–617, Dec 2007.

[22] Y. He, KH. Yap, L. Chen, and L-P Chau, "A nonlinear least square technique for simultaneous image registration and super-resolution," *Image Processing, IEEE Transactions on*, vol. 16, no. 11, pp. 2830–2841, 2007.

[23] S. Villena, M. Vega, S.D. Babacan, R. Molina, and A.K. Katsaggelos, "Bayesian combination of sparse and non-sparse priors in image super resolution," *Digital Signal Processing*, vol. 23, no. 2, pp. 530–541, 2013.

[24] Michael B Wakin, Jason N Laska, Marco F Duarte, Dror Baron, Shriram Sarvotham, Dharmpal Takhar, Kevin F Kelly, and Richard G Baraniuk, "An architecture for compressive imaging," in *Image Processing, 2006 IEEE International Conference on*. IEEE, 2006, pp. 1273–1276.